CCA-756

541.18:546.212:541.45
Conference Paper

Water on Oxide Surfaces*

A. C. Zettlemoyer and [a]E. McCafferty

Center for Surface and Coatings Research, Lehigh University, Bethlehem, Pennsylvania, and [a]Metallurgy Division, Naval Research Laboratory, Washington, D. C., U.S.A.

Received November 20, 1972

Most oxide surfaces interact with ambient water vapor to form a layer of chemisorbed hydroxyls. Physical adsorption of multilayer water readily starts by hydrogen bonding onto the hydroxyl array. The normally hydrophilic surface of silica can be modified by heating to produce a predominantly hydrophobic matrix which contains but a few isolated hydrophilic sites, around which water adsorbs in clusters. The authors' results on both hydrophilic and hydrophobed oxides are discussed and compared to results in the literature.

INTRODUCTION

The interaction of water vapor with oxide surfaces is important in many diverse problems, ranging from the growth of corrosion products on structural metals, to cloud seeding, to the dispersion of paint pigments. It is widely known that water vapor in the atmosphere chemisorbs on most metal oxides to form hydroxyl groups. Evidence[1] for the presence of surface hydroxyls is derived from infrared spectroscopy, exchange reactions, weight loss studies, and high heats of immersion. These surface hydroxyls can be removed by heating, as in Fig. 1, although the rehydration process is not always reversible. In the case of silicas heated above 400 °C, rehydration of the siloxane groups, Fig. 1, I → II,

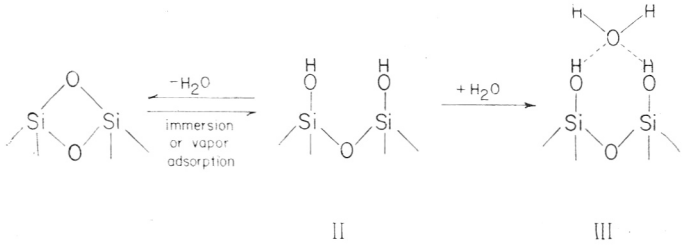

Fig. 1. Dehydration and rehydration of a silica surface.

is slow and incomplete[2]. That is to say, the normally hydrophilic silica surface, Fig. 1-II, can be treated to make a hydrophobic substrate containing but a few isolated hydroxyl groups. This paper will consider the interaction of water vapor with both types of oxide surfaces: those containing a few hydrophilic sites in a hydrophobic matrix, and those entirely hydroxylated.

* Based on a lecture presented at the *III International Summer School on the Chemistry of Solid/Liquid Interfaces*, Rovinj, Yugoslavia, July 1—5, 1972.

HYDROXYLATED SURFACES

Under normal conditions, the oxide surface will be completely hydroxylated due to interaction with ambient water vapor in the environment. We consider this type of surface first.

»Hard« and »Soft« Hydroxyls

Much effort has been expended by many investigators to characterize oxide surfaces in terms of *(1)* the energetics of dehydration, and *(2)* the surface population of hydroxyl groups. The ease or difficulty of dehydration can be followed by the heat of immersion as a function of pretreatment temperature. The picture was made clear first in the case of silica, described in part above. Fig. 2, redrawn from the work of Young and Bursch[2], shows the heat of immersion to be constant up to an outgassing temperature of 180 °C, because only physically adsorbed water is removed during pretreatment and adsorbed during immersion. Above 180 °C, the heat of immersion increases due to the re-adsorption of expelled chemisorbed hydroxyls, Fig. 1 (I $\gtrless$ II). As noted earlier, when the silica is heated above 400 °C, the siloxane groups become more stable, and rehydration is slow and incomplete within the time of the experiment, so that the heat of immersion decreases.

Other oxides behave differently. With γ-Al_2O_3[3], α-Fe_2O_3[4], and ThO_2[5], there is no maximum, but a monotonic increase in the heat of immersion with outgassing temperature (See Fig. 3.). This type of curve indicates that these oxides

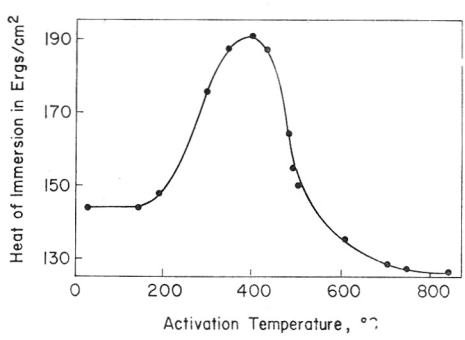

Fig. 2. Heat of immersion of silica in water as a function of outgassing temperature. (Redrawn from Young and Bursch[2]).

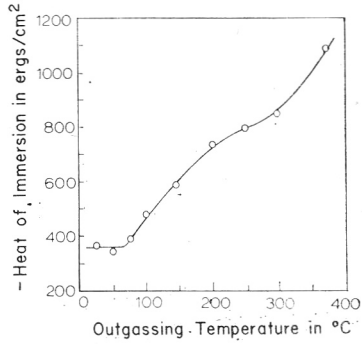

Fig. 3. Heat of immersion of α-Fe_2O_3 in water as a function of outgassing temperature. (Zettlemoyer and McCafferty[4]).

are easily and reversibly rehydrated, in contrast to SiO_2. Thus, the hydroxyls on α-Fe_2O_3 may be termed »soft« compared to the »hard« hydroxyls on SiO_2, because in the former case the hydroxyls are not only the easier lost (75° *vs.* 180° outgassing temperatures) but the easier regained after more drastic outgassings. More will be said later about heats of immersion.

Hydroxyl Coverage

The concentration of surface hydroxyls has been determined by a variety of techniques including application of BET theory to water vapor adsorption[6–10], D_2O exchange[11,12], replacement reactions with specific reagents[12], and NMR

techniques[13]. Some results from the literature are compiled in Table I, with the maximum concentration of surface hydroxyls recalculated in terms of OH's/100 Å² if not given so in the original paper. Table I is not intended to be a complete survey but does show the surface concentration is generally 5—10 hydroxyls per 100 Å². Gammage, Fuller, and Holmes[16] recently reported an unusually high value of 36 OH's/100 Å² for a non-porous thoria, far in excess of the amount expected from crystallographic calculations, but there was a possibility of a bulk reaction in that study.

TABLE I

Total Concentration of Surface Hydroxyl Groups

Oxide	Number OH groups /100 Å²	Investigators	Method
ZnO	6.8—7.5	Nagao[6]	BET
SiO_2	4.8	Davydov *et. al.*[11]	D_2O exchange
	4.2	Burmudez[13]	NMR
	4.6	de Boer and Vleeskens[14]	Weight loss
TiO_2 (anatase)	6.2	Jurinak[7]	BET
(anatase)	4.9	Boehm[12]	D_2O exchange
(rutile)	8.5	Hallabaugh an Chessick[8]	BET
(rutile)	2.7—7.1*	Boehm[12]	D_2O exchange
α-Fe_2O_3	4.6—7.9*	Morimoto *et al.*[9]	BET
	5.5	McCafferty and Zetlemoyer[10]	BET
α-Al_2O_3	15	Morimoto *et al.*[15]	Volume water lost upon heating
γ-Al_2O_3	10	Morimoto *et al.*[15]	
η-Al_2O_3	4.8	Boehm[12]	CH_3MgI (CH_4 evolution)

* For different samples.

The concentration of surface hydroxyls is important as these species provide sites for the initiation of multilayer adsorption of water molecules.

Adsorption on the Hydroxylated Surface

Kiselev[17] proposed that water adsorption on the hydroxylated substrate occurs by hydrogen bonding between the oxygen on water and two underlying surface hydroxyls, as in Fig. 1-III. Different sorts of evidence infer that this is the case. First, BET V_m's for water on TiO_2[8,9] and on α-Fe_2O_3[9] yielded 1 physically adsorbed water molecule per 2 surface OH's. In each case, an initial BET V_m for water on the dehydroxylated surface included the amount of surface hydroxyls re-formed plus the amount of companion physical adsorption. The physisorbed amount was removed by evacuation and then determined by a second V_m. The difference in the two V_m's gave the amount in the chemisorbed monolayer, and hence the ratio n (H_2O) : n (OH).

Convincing evidence that this mode of adsorption is operative on hydroxylated α-Fe_2O_3 has been given recently in several ways. McCafferty, Pravdić, and Zettlemoyer[10,18] reported that the physisorbed monolayer caused no change in the dielectric constant, ε', as shown in Fig. 4. This behavior means that water molecules in the physisorbed monolayer are localized on the hydroxyls and cannot orient with the alternating applied field. Hence, the localized

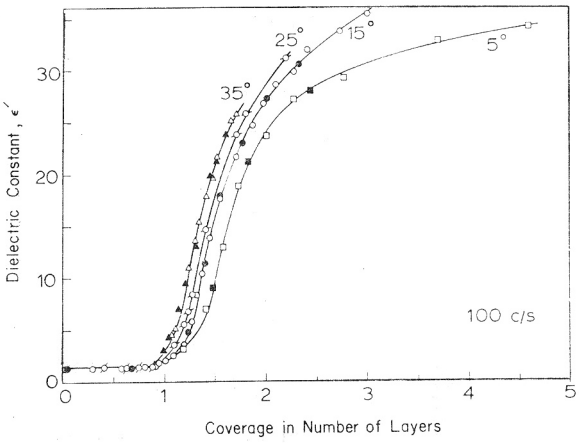

Fig. 4. Dielectric constant at 100c/s for water vapor at 25 °C on hydroxylated α-Fe_2O_3. Solid points indicate the desorption branch. (McCafferty, Pravdić, and Zettlemoyer[18]).

monolayer does not contribute to the capacitance of the system. This behavior is consistent with double hydrogen bonding of water molecules to the substrate, as in Fig. 1-III. The dielectric constant rises sharply in the second layer, where the adsorbate is more mobile. Here, a temperature increase causes an increase in dielectric constant as thermal excitation begins to overcome the ordering effect of the oxide surface. Within the monolayer, however, where the molecules are more tightly bound, a temperature increase of 30 °C does not assist the adsorbate in orienting with the alternating field.

A second explanation for the fixed dielectric constant in the monolayer (Fig. 4) can be suggested, but quickly eliminated. If the molecules in the statistical monolayer were arranged in clusters, there would be no increase in ε' until the gaps between clusters were bridged into a continuous network by the »second« BET layer. However, cluster formation on a predominantly hydroxyl-covered surface is not likely. The formation of clusters requires a few isolated hydrophilic sites in a hydrophobic matrix, as was demonstrated for water on AgI[19]. Moreover, a single relaxation time would not be expected if water clusters and thinner bridges coexisted on the surface, but instead each of the two structures should exhibit a different relaxation time. However, the observed[18] Cole-Cole plots were simple arc plots rather than overlapping and double-humped[20].

Heats of adsorption also point to double hydrogen bonding for the physically adsorbed monolayer. The net differential heat of adsorption from the vapor determined by differentiation of the heat of immersion *vs.* precoverage curve

gave a value of about 10 kcal/mole for the onset of adsorption on the hydroxylated surface[10]. This value corresponds approximately to two hydrogen bonds. A similar result was obtained for the water-thoria system[21].

Added evidence that monolayer water is localized on hydroxylated α-Fe_2O_3 was given on an entropy basis[22]. The experimental integral entropy of adsorption obtained from multitemperature isotherms agreed with that calculated from statistical thermodynamics for an immobile film, but not with that calculated for a mobile one.

Structuring of Adsorbed Water

A most interesting observation with α-Fe_2O_3 was that the physically adsorbed water developed in an ordered, hydrogen bonded structure in the first few layers[18]. Characteristic relaxation times τ_0 were calculated from Cole-Cole arc plots of dielectric constant ε' *vs.* dielectric loss ε'', illustrated in Fig. 5 and described by:

$$\log \left| V/U \right| = (\alpha - 1) \log 2\pi f + (\alpha - 1) \log \tau_0 \qquad (1)$$

where U and V are the arc chords shown in Fig. 5, α is a parameter giving the skewness from ideal Debye behavior, and f is the applied frequency. (Each data point in Fig. 5 corresponds to a different frequency from 70 c/s to 300 kc/s.) Plots of $\log \left| V/U \right|$ against $\log 2\pi f$ yield α and τ_0. For more detail, see Refs. 10 and 18.

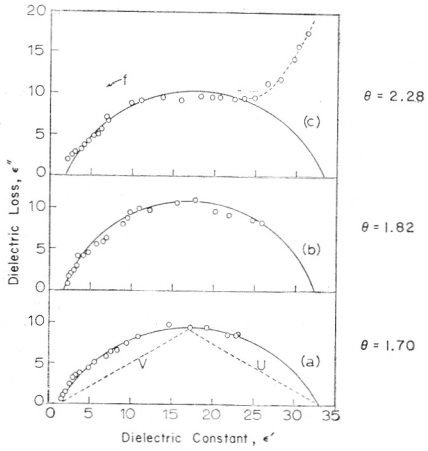

Fig. 5. Cole-Cole arc plots for several coverages of water vapor on hydroxylated α-Fe_2O_3 at 15 °C: (*a*) $\Theta = 1.70$, $f_{char} = 176$c/s; (*b*) $\Theta = 1.82$, $f_{char} = 284$c/s; (*c*) $\Theta = 2.28$, $f_{char} = 1.09$kc/s. (McCafferty, Pravdić, and Zettlemoyer[18]).

The results are shown in Fig. 6 in terms of characteristic frequencies, $f_{char} = 1/(2\pi\tau_0)$. Coverages refer to the number of layers of physisorbed water on the hydroxylated surface. At about three layers, the characteristic relaxation frequencies for the system approach 10 kc/s. This frequency corresponds to the characteristic relaxation frequency of ice, if extrapolated up to 25°, and is seven decades lower than the characteristic frequency of liquid water[23]. That this value of 10 kc/s is characteristic of a hydrogen bonded »ice-like« solid

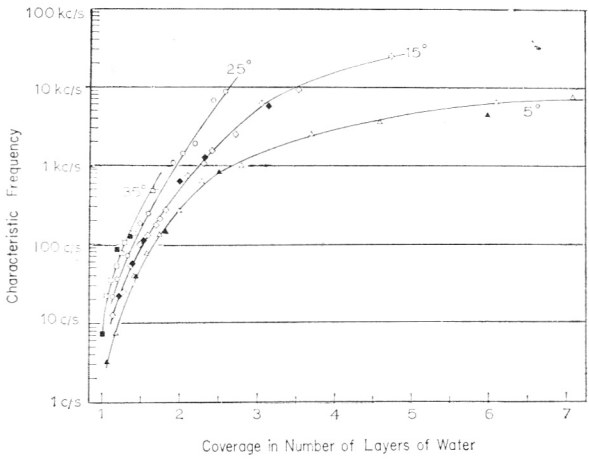

Fig. 6. Characteristic frequency of adsorbed water vapor on hydroxylated α-Fe_2O_3 as a function of coverage. Solid points indicate desorption. (McCafferty, Pravdić, and Zettlemoyer[18]).

could it persist at 25 °C must mean that the adsorbate has developed stronger hydrogen bonding than liquid water, and the adsorbed molecules have a restricted rotation to some extent like that in ice. Said simply, the adsorbate is »ice-like« or structured.

The smooth increase in characteristic frequency with coverage in Fig. 6 suggests that the structuring process is a gradual one. As discussed earlier, the first physisorbed layer is localized by hydrogen bonding of a single water molecule to two surface hydroxyls. That molecules in the second layer must be less constrained follows from the abrupt rise in ε' in Fig. 4. If this layer is on the average singly hydrogen bonded to the underlying first layer, rotational freedom will be provided for response to the a. c. field ,and yet some ordering of the adsorbate by the solid surface will be preserved. This second layer will become more ordered when hydrogen bonded to a third layer, and so on, until the ordering effect of the surface is overcome and liquid layers are formed.

Added support for this model has been given by Hair and Hertl[24] in a different way for silica surfaces. These authors prepared a surface consisting of only vicinal hydrogen bonded hydroxyls. The water vapor adsorption isotherm showed two steps, the first at 1 water molecule/OH pair, indicative of double hydrogen bonding. The second step occurred at 3 molecules/OH pair, which was accounted for by single hydrogen bonding of two more water molecules to the first.

Other evidence for organization of adsorbed water vapor at solid surfaces has been summarized elsewhere[18] and need not be repeated here. Whether such ordered films persist from solution would appear to depend on the position of the oxide from its pzc[25].

Heterogeneities, Difficulties, and Discrepancies

A very real problem which plagues the use of powder samples is the uncertainty that data for some particular sample are truly representative of that oxide surface in general. Observations made with powder samples very often depend on such factors as surface heterogeneities, degree of surface

crystallinity, porosity, particle size, purity, and even on the history of the sample. Thus, there is often contradiction or in the very least confusion in comparing results from oxide to oxide or from laboratory to laboratory.

Graphic examples are provided by some recent heat of immersion work. Some TiO_2 samples displayed maxima[26,27] in the heat of immersion as a function of outgassing temperature while others did not[28,29]. For anatase TiO_2, a sample of low surface area (large crystallites) showed a maximum, but not samples of high surface area (smaller crystallites)[28]. The authors suggested that surfaces with a lower crystallinity are more easily hydrated due to a strained

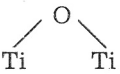

structure.

Morimoto and coworkers[30] found that two out of four of their α-Fe_2O_3 samples gave a maximum in immersional heat *vs.* outgassing temperature. No explanation was given. The maxima which did occur were at temperatures higher than those used in Fig. 3, but there might have been loss of surface oxygens at these higher temperatures[4].

Porosity is also an important factor. Holmes and coworkers[31] recently suggested that similar maxima observed for some (but not all) ZrO_2 samples was due in part to slow diffusion of water into pores. These workers also observed that the heat of immersion increased with increasing surface area (*i. e.,* decreasing crystallite site) in disagreement with the opposite trend observed by Wade and Hackerman[3,26]. In the Wade and Hackerman work, the smaller crystallite size, *i. e.,* more nearly amorphous surface yielded the smaller heat. But Holmes and coworkers suggest that their particular method of sample preparation produced a less heterogeneous surface along with a smaller surface area.

With regard to water vapor adsorption, there is some evidence to dispute the model discussed earlier involving double hydrogen bonding on the hydroxyls. Boehm[32] reports $n(H_2O) : n(OH)$ to be 1 : 1 water on silica, and η-alumina. This ratio would suggest that one water molecule is *singly* hydrogen bonded onto one OH group. Nagao[33] observed one water molecule per surface hydroxyl on ZnO, but the adsorption isotherms always displayed a peculiar »hump« at moderate relative pressures. Thermodynamic evidence suggested that the surface hydroxyls produced a partially homogeneous surface with two types of sites for physical adsorption. However, in another study[34] on ZnO, no »humps« were observed in the adsorption isotherms. Water areas were not given, but we calculated BET areas taking data from the published figures (admittedly a risky practice), and got 1 H_2O/2 surface OH's, in agreement with results discussed earlier for water on α-Fe_2O_3, TiO_2, ThO_2, and SiO_2.

HYDROPHILIC SITES IN A HYDROPHOBIC MATRIX

There is no doubt that sometimes such hydrophilic sites are detrimental to the utility of the hydrophobic material. Take water repellency of a cloth: Hydrophilic areas could easily form the route to the passage of water. Surprisingly, at first glance, such sites can produce beneficial or useful effects. Take the lubricity of graphite: it is the water cluster around the hydrophilic sites that gives it utility in commutator brushes, and the like. Take the adhesion of

organic coatings and printing ink to polyethylene packaging film: the surface of the film is treated so that polar sites are purposely produced by chemical action to enhance adhesion. Take ice nucleants such as nature provides to »seed« clouds and thus cause rainfall, or as might be artfully introduced: in »cloud seeding«, the first water molecules to adsorb go down on these polar sites and then the next adsorbate molecules cluster around these. The embryo thus formed, probably after it grows past the critical radius at which the bulk free energy change can counteract the surface free energy increase, goes over to ice, the stable phase at the ambient temperatures of clouds. It is the curious thermodynamic properties of these polar site/adsorbate interactions on such otherwise hydrophobic surfaces which will be discussed here.

The surface concentration of these polar sites can vary enormously. On Graphon, a graphitized carbon black of 100 $m^2/g.$, about one in 1500 surface sites is polar and accepts highly polar adsorbates like water. On Teflon 6, a polytetrafluoroethylene about one in 200. On silver iodide, the surface concentration varies considerably with the preparation, but it is often about one in four surface sites. The work at Lehigh University seems to show that the contact angles of water on pressed discs of these powders agree with those obtained on the purest single crystals of film. At fairly high surface concentrations of polar sites as on treated polyethylene film, the contact angle of water was indeed found to decrease, but no relationship with the amount of treatment nor performance in adhesion could be found. Adsorption and heat of immersion measurements, however, are successful in characterizing these sites.

Fifteen years ago, we were studying[35] water adsorption on Graphon. In the early sixties, the earlier findings proved useful in studying and in producing synthetic ice nucleants[19]. But let us go back to an earlier date. In the late forties, Vonnegut[36] and Langmuir chose silver iodide as a »cloud seeder« on the basis that the common basal planes matched ice closely, and considering that epitaxy was important to the nucleation process. Silver iodide, even though expensive, remains the most effective readily available nucleant and is easily dispersed by burning acetone solutions. Nevertheless, silver iodide is highly insoluble in water and the really pure solid surface would not be expected to adsorb water. Early reports[37] on the adsorption of water on silver iodide incorrectly claimed close-packed multilayer adsorption. Apparently, these workers used silver iodide prepared from ammonium iodide, and they got absorption as well as adsorption. Indeed a trend toward lower water adsorption with purer samples has been reported[38], but a really pure surface as might be produced from silver and iodine under UHV has not been examined.

At least one of our substitute nucleants rivals silver iodide in efficiency tests in a cloud chamber[19] (See Fig. 7). No exhaustive attempts to synthesize nucleants have been made. Instead, we have been interested in learning how nucleants work, and thus the required surface properties. Most of our synthetic nucleants have been made by hydrophobing silicas, that is, by proceeding in a direction which offhand would be expected to be opposite to that required. Besides the fact that silicas are inexpensive, their surface properties have been explored more completely than those of any other oxide. The Lehigh work will be reviewed here and some recent developments will be included.

Water adsorption isotherms at several temperatures on Graphon[39], AgI[40], and dehydrated HiSil No 2[41] are presented in Figs. 8—10. Such reversible isotherms displaying increasing amounts adsorbed with increasing temperatures

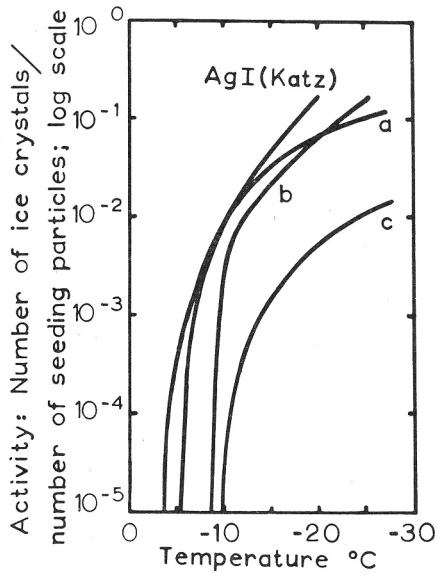

Fig. 7. Ice-nucleating ability of silver iodide and hydrophobed silicas. (*a*) A silica heated with $AgNO_3$ to 650 °C compares favorably with the classical efficiency curve due to Katz for AgI; (*b*) a heat-treated silica made from (*c*) wet-precipitated silica. At low enough temperatures, all particles become nucleants.

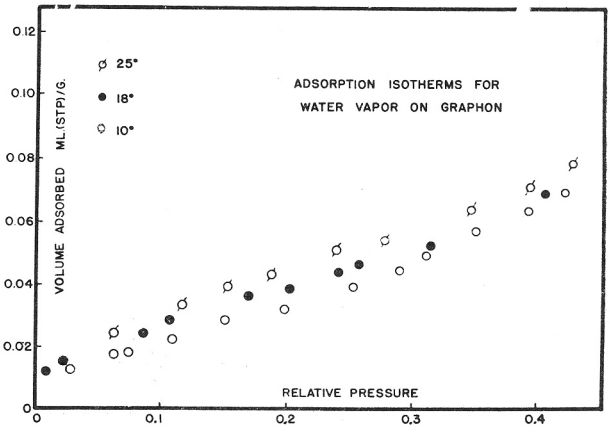

Fig. 8. Volume of water vapor adsorbed onto Graphon as a function of relative pressure at three temperatures. The isotherms are completely reversible. The increased adsorption with increased temperature was quite unusual when first reported.

were reported earlier by Lamb and Coolidge[42] for water on charcoal, but in this case the porosity complicates matters. This curious phenomenon leads to an interesting coherent set of thermodynamic properties. The following results are required if reversible isotherms fall in this reverse order to that usually expected:

1) The isosteric heat of adsorption is less than the heat of liquefaction. Curves for the H_2O/Graphon system are shown in Fig. 11. Model isotherms

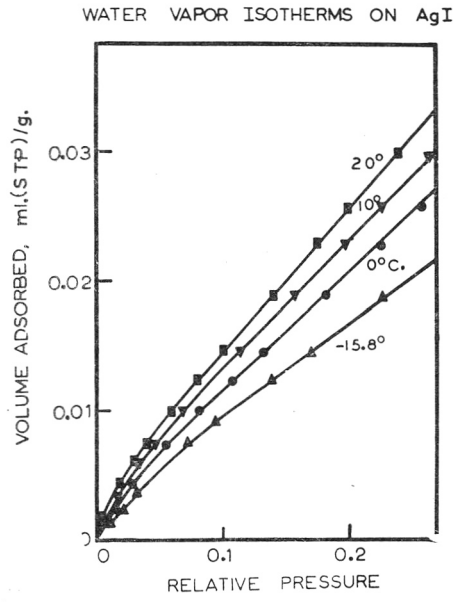

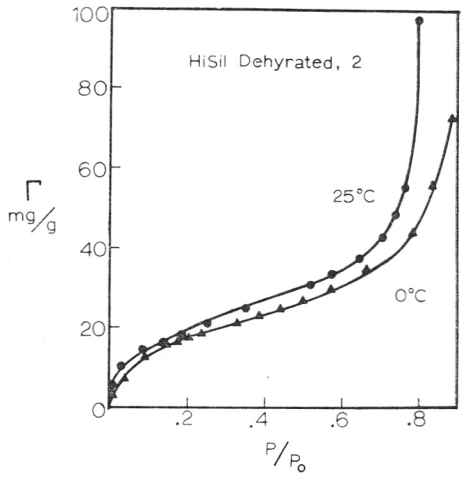

Fig. 9. Volume of water vapor adsorbed onto silver iodide as a function of relative pressure at low temperatures. Again, increased adsorption with increase in temperature. Impurity sites are thought to be responsible for the water adsorption by their water insoluble and hence hydrophobic compounds.

Fig. 10. Volume of water vapor adsorbed onto dehydrated HiSil as a function of relative pressure at two temperatures. Here is a »synthetic« nucleant which shows the same water adsorption behavior as do AgI and Graphon.

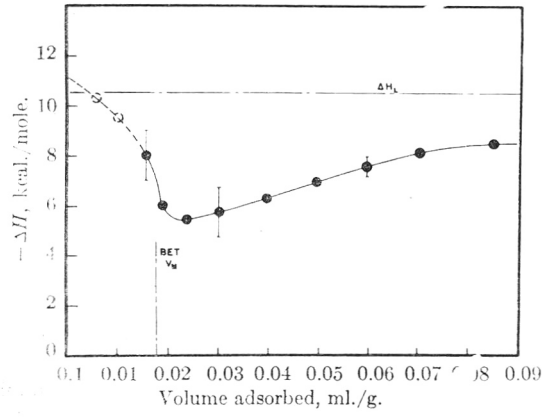

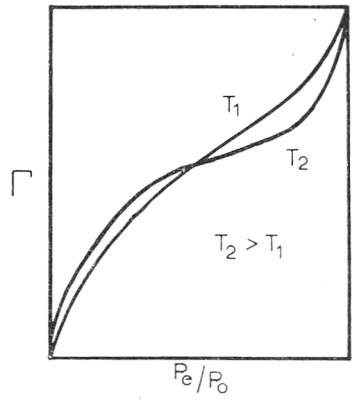

$$\ln \frac{P_2}{P_1} = \ln \frac{(P_e/P_o)_2 (P_o)_2}{(P_e/P_o)_1 (P_o)_1} = \frac{q_{st}}{R} \left[\frac{T_2 - T_1}{T_1 T_2} \right]$$

$$\Delta h_{ads} = \int_0^{\Gamma} q_{st}\, d\Gamma = \left[h_{i(sL)} - h_{i(sfL)} \right] + \Gamma \Delta H$$

Fig. 11. The variation in the isosteric heat calculated from the Clapeyron-Classius equation with increasing coverage for adsorption of water on Graphon. Note that the value of the heat of adsorption is lower that the heat of liquefaction at all coverages.

Fig. 12. Hypothetical »cross-over« isotherm used to show the thermodynamic significance of the temperature dependence of adsorption isotherms. Below the »cross-over«, the q_{st} is lower than the heat of liquefaction, and the heat of immersion rises with precoverage.

which cross are shown in Fig. 12. We can write from the Clapeyron-Clausius equation:

$$\ln \frac{P_2}{P_1} = \ln \frac{(P_e/P_0)_2 (P_0)_2}{(P_e/P_0)_1 (P_0)_1} = \frac{q_{st}}{R} \left(\frac{T_2 - T_1}{T_1 T_2} \right). \quad (1)$$

Therefore, at the crossover point, q_{st} is just the heat of liquefaction. Below this point, q_{st} is less than the heat of liquefaction: above, it is greater as is usual.

2) The entropy of the adsorbed phase is high as shown for the water/Graphon system in Fig. 13. To calculate these entropies all the changes were ascribed to the adsorbate; this assumption is reasonable for this weak adsorption. The »Hill hypothesis« has it that the differential entropy should cross the minimum in the integral entropy at the monolayer value[43]. Interestingly, the BET value for water, only 1/1500 the nitrogen monolayer capacity, agrees well with the estimate from the entropies. For AgI, this agreement was not found[40].

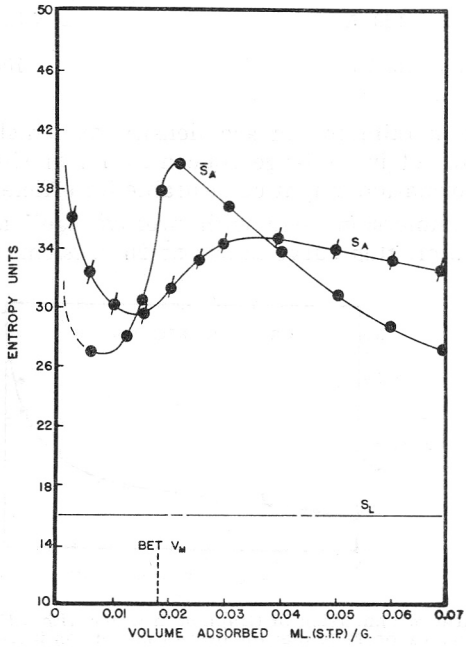

Fig. 13. Plots of the differential and integral entropies, $\bar{S}_s$ and S_s, respectively, as a function of the volume of water adsorbed.

The low-energy adsorption and the high entropy both indicate high mobility of the adsorbed water molecules. It is interesting to take the entropy values for the »nominal« first layer on Graphon and on a particular sample of AgI, which happens to be 29.3 eu in both cases (See Table II). Following Graham[44], the translational part can be estimated by subtracting out the other contributions. Then, the two-dimensional partition function can be used to calculate the surface area over which the adsorbed molecule migrates on the average. The result is 120 A^2 in both cases. For Graphon, the polar site density is so small that there is no lateral interaction. The AgI sample studied, on the

TABLE II

Entropy of Water on Hydrophobic Surfaces

$$Q_t = \frac{2\pi m k T}{h^2} a$$

$$S_t = R\left[1 + \ln \frac{2\pi m k T}{h^2} a\right]$$

Graphon		AgI
Observed S, eu	29.3	29.3
Config. 1.0		
Rot. 8.4		
Vib. 2.6		
	12.0	12.0
Residual, trans.	17.3	17.3
a = 120 Å²		a = 120 Å²
Available: 16,000		100

other hand, has the maximum surface density at which lateral interaction would be expected to set in. A large concentration of sites, still isolated sufficiently for cluster formation, might be desirable for efficiency in ice nucleation.

3) The heat of immersion rises with precoverage[35] as shown in Fig. 14. For Graphon into water, this curve starts at 26 ergs/cm² and is still far from

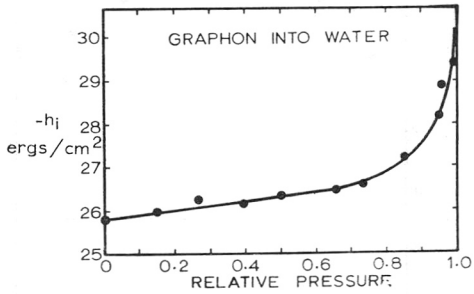

Fig. 14. Variation of the heat of immersion of Graphon in water with different precoverages of the Graphon surface with water vapor. Note that the heat of immersion increases as the surface of the Graphon adsorbes more water vapor. This shows that the bare surface of the Graphon has less affinity for water than does the adsorbed water

118.5 ergs/cm², which is the surface enthalpy of liquid water, at 0.99 relative pressure. This unusual requirement of a rising heat of immersion isotherm is indicated by the equation:

$$h_{ads} = (h_{i(SL)} - h_{i(sfL)}) + h_L \qquad (2)$$

All these terms are minus quantities. This integral heat of adsorption from the vapor (the left hand term) is less than the heat of liquefaction when $h_{i(SfL)}$ is greater in magnitude than $h_{i(SL)}$. Enthalpywise, then, water prefers the partially precovered surface to the bare surface.

These facts reveal much about the nature of adsorption of water on the polar heterogeneities on a hydrophobic surface. Such surfaces, like silver iodide or partially hydrophobed silicas (by burning) are catalysts for ice nucleation (rain making) in clouds. They will not be discussed in detail here.

Reflectance IR

Many workers have used pressed discs of powdered samples to determine infrared spectra by passage of the radiation through the disc and recording the resulting bands in the principle OH stretch region 3740—3400 cm^{-1}. The isolated hydroxyl peak is at 3740 cm^{-1} and nearby absorptions represent interacting neighbor hydroxyls. Trouble is the excessive scattering as the IR beam passes through the disc coupled with the energy absorption and consequent temperature rise. Thus, adsorption of water vapor is considerably less than expected from the apparent temperature and the relative humidity to which the sample is exposed. For these reasons we turned to reflectance spectroscopy in the near IR. When employed with monochromatic radiation, temperature rise is less than 0.1 ^{0} C.

The experimental arrangment is shown as developed by Professor K. Klier at Lehigh in Fig. 15. And in Fig. 16, the peak for the bare surface of a partially

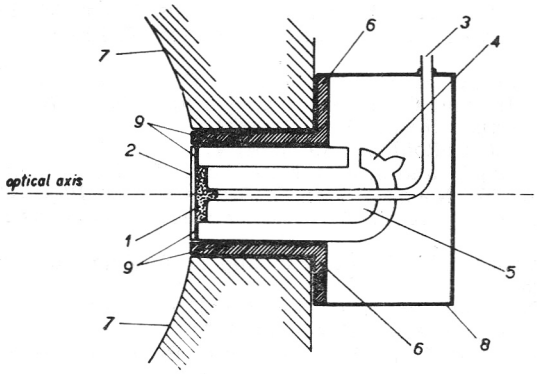

Fig. 15. A vacuum cell for reflectance spectra measurements at various temperatures. *1*, Sample; *2*, quartz window; *3*, gas inlet and vacuum; *4*, vacuum jacket; *5*, vessel for thermostatting liquid; *6*, metal holder; *7*, integrating sphere; *8*, light shielding; *9*, Araldite joints.

hydrophobed silica is shown at 7480-cm^{-1} for the 2γ or overtone band. It decreases with water adsorption and the broader band at somewhat lower frequencies increases. The combination band $(\gamma + \delta)$ for molecular water increases as the water adsorption occurs. The work of Luck[45] for bulk water and ice in the same region is particularly important because it shows that the adsorbed water is not the same as the bulk water.

It is hoped that we can observe ice nucleation through this reflectance IR technique as it occurs on the nucleant surface. Already we know that ice does not form around the hydrophilic sites at four to six nominal monolayers. It is not unexpected that such »two dimensional« ice does not form.

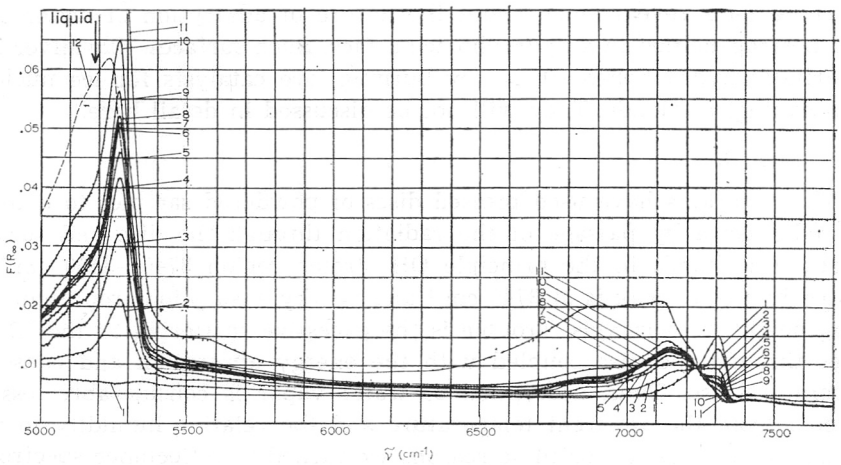

Fig. 16. Near-IR spectra of water adsorbed on partially hydrophobed silica. No. 1 is for the bare surface and then surface concentration of water is increased gradually.

REFERENCES

1. Detailed references can be found in M. L. Hair, *Infrared Spectroscopy in Surface Chemistry,* Marcel Dekker, New York, 1967, Chapts. 4, 5.
2. G. J. Young and T. P. Bursch, *J. Colloid Sci.* **15** (1960) 361.
3. W. H. Wade and N. Hackerman, *J. Phys. Chem.* **64** (1960) 1196.
4. A. C. Zettlemoyer and E. McCafferty, *Z. Physik. Chem. N.F.* (Frankfurt) **64** (1969) 41.
5. H. F. Holmes and C. H. Secoy, *J. Phys. Chem.* **69** (1965) 151; H. F. Holmes, E. L. Fuller, Jr., and C. H. Secoy, *J. Phys. Chem.* **70** (1966) 436.
6. M. Nagao, *J. Phys. Chem.* **75** (1971) 3822.
7. J. J. Jurinak, *J. Colloid Sci.* **19** (1964) 477.
8. C. M. Hollabaugh and J. J. Chessick, *J. Phys. Chem.* **65** (1961) 109.
9. T. Morimoto, M. Nagao, and F. Tokuda, *J. Phys. Chem.* **73** (1969) 243.
10. E. McCafferty and A. C. Zettlemoyer, *Discussions Faraday Soc.* No. 52 (1972).
11. V. Ya. Davydov, A. V. Kiselev, and L. T. Zhuravlev, *Trans. Faraday Soc.* **60** (1964) 2254.
12. H. Boehm, *Discussions Faraday Soc.* No. 52 (1972).
13. V. M. Burmudez, *J. Phys. Chem.* **74** (1970) 4160.
14. J. H. de Boer and J. M. Vleeskens, *Proc. Kon. Ned. Akad. Wetenasch,* **B 61**, **2** (1958).
15. T. Morimoto, K. Shiomi, and H. Tanaka, *Bull. Chem. Soc. Jap.* **37** (1964) 392.
16. R. B. Gammmage, E. L. Fuller, Jr., and H. F. Holmes, *J. Phys. Chem.* **74** (1970) 4276.
17. A. V. Kiselev in *Structure and Properties of Porous Materials,* D. H. Everett and F. S. Stone, Eds., Academic Press, New York, 1958, p. 195.
18. E. McCafferty, V. Pravdić, and A. C. Zettlemoyer, *Trans. Faraday Soc.* **66** (1970) 1720.
19. A. C. Zettlemoyer, N. Tcheurekdjian, and C. L. Hosler, *Z. angew. Mat. Phys.* **14** (1963) 496.
20. See, for example: H. Kilp, S. K. Garg, and C. P. Smyth, *J. Chem. Phys.* **45** (1966) 2799.
21. H. F. Holmes, E. L. Fuller, Jr., and C. H. Secoy, *J. Phys. Chem.* **72** (1968) 2095.
22. E. McCafferty and A. C. Zettlemoyer, *J. Colloid Interface Sci.* **34** (1970) 452.
23. C. P. Smyth, *Dielectric Behavior and Structure,* McGraw-Hill, New York, 1955, p. 70.

24. M. L. Hair and W. Hertl, *J. Phys. Chem.* **73** (1969) 4269.
25. See *Discussion Remarks*, J. P. Quirk and E. S. Hall in *Discussions Faraday Soc.* No. **52** (1972), regarding Ref. 10.
26. W. H. Wade and N. Hackerman, *J. Phys. Chem.* **65** (1961) 1681.
27. T. Morimoto, M. Nagao, and T. Omori, *Bull. Chem. Soc. Jap.* **42** (1969) 943.
28. T. Omori, J. Imai, M. Nagao, and T. Morimoto, *Bull. Chem. Soc. Jap.* **42** (1969) 2198.
29. A. C. Zettlemoyer, R. D. Iyengar, and P. Scheidt, *J. Colloid Interface Sci.* **22** (1966) 172.
30. T. Morimoto, N. Katayama, H. Naono, and M. Nagao, *Bull. Chem. Soc. Jap.* **42** (1969) 1490.
31. H. F. Holmes, E. L. Fuller, Jr., and R. B. Gammage, *J. Phys. Chem.* **76** (1972) 1497.
32. H. Boehm, *Discussion Remarks* in *Discussions Faraday Soc.* No. 52 (1972).
33. M. Nagao, *J. Phys. Chem.* **75** (1971) 3822.
34. M. M. Egorev, N. N. Dobrovol'skii, V. F. Kiselev, G. F. Furman, and V. Khrustaleva, *Russ. J. Phys. Chem.* **39** (1965) 1939.
35. A. C. Zettlemoyer, G. J. Young, J. J. Chessick, and F. H. Healey, *J. Phys. Chem.* **57** (1953) 649.
36. B. J. Vonnegut, *J. Appl. Phys.* **18** (1947) 593.
37. S. J. Birstein, *J. Meteorol.* **12** (1954) 324.
38. M. L. Corrin, H. W. Edwards, and J. A. Nelson, *J. Atmospheric Sci.* **21** (1964) 565.
39. D. R. Bassett, *Ph. D. Thesis*, Lehigh University, Center for Surface and Coatings Research, Bethlehem, Pennsylvania, 1967.
40. N. Tcheurekdjian, A. C. Zettlemoyer, and J. J. Chessick, *J. Phys. Chem.* **68** (1964) 773.
41. W. C. Hamilton, Private communication.
42. A. S. Coolidge, *J. Am. Chem. Soc.* **49** (1927) 708.
43. T. L. Hill, P. H. Emmett, and L. G. Joyner *J. Am. Chem. Soc.* **73** (1951) 5102.
44. D. Graham, *J. Phys. Chem.* **60** (1956) 1022.
45. W. A. P. Luck, *Ber. Bunsenges. Phys. Chem.* **69** (1965) 626.

IZVOD

Voda na površinama oksida

A. C. Zettlemoyer i E. McCafferty

Interakcija vodene pare s površinama oksida važan je fizikalno-kemijski proces u mnogim područjima znanosti i tehnologije, od rasta korozionih slojeva na konstruktivnim metalima, preko metereološke primjene u nukleaciji oblaka, do problematike dispergiranja pigmenata u industrijskim premazima.

U ovom radu obrađeni su primjeri »meko« i »tvrdo« hidroksiliranih površina primjerima podataka dobivenih o energetici hidratacije i dehidratacije i o površinskoj koncentraciji hidroksilnih grupa. Primjer »tvrdo« hidroksilirane površine pokazan je na SiO_2 (amorfna silika), a »meko« na α-Fe_2O_3. Usporedbeni podaci pokazani su za Graphon (grafitiziranu čađu), AgJ, Al_2O_3 i TiO_2. Eksperimentalni podaci na osnovu kojih su izračunate entropija i entalpija vode na površinama dobiveni su kalorimetrijski, mjerenjem toplina kvašenja, mjerenjem dielektričke disperzije, tehnikom mjerenja reflektiranih IR spektara.

CENTER FOR SURFACE AND COATINGS RESEARCH
LEHIGH UNIVERSITY, BETHLEHEM, Pa., U.S.A.
i
NAVAL RESEARCH LABORATORY
WASHINGTON, D. C., U.S.A.

Primljeno 20. studenoga 1972.